ARTICLE

Ultrafast Growth of Highly Branched Palladium Nanostructures for Catalysis

John Watt,[†] Soshan Cheong,[†] Michael F. Toney,[‡] Bridget Ingham,[§] James Cookson,[⊥] Peter T. Bishop,[⊥] and Richard D. Tilley[†,*]

[†]Victoria University of Wellington MacDiarmid Institute of Advanced Materials and Nanotechnology, Kelburn Pde, Wellington, New Zealand, [‡]Stanford Synchrotron Radiation Laboratory, 2575 Sand Hill Road, Menlo Park, California 94025, [§]Industrial Research Limited MacDiarmid Institute of Advanced Materials and Nanotechnology, 69 Gracefield Road, Lower Hutt, New Zealand, and [⊥]Johnson Matthey Technology Centre, Blount's Court, Sonning Common, Reading, RG4 9NH, U.K.

ABSTRACT Palladium is widely used as a catalyst in pharmaceutical and chemical syntheses as well as in the reduction of harmful exhaust emissions. Therefore, the development of high performance palladium catalysts is an area of major concern. In this paper, we present the synthesis of highly branched palladium nanostructures in a simple solution phase reaction at room temperature. By varying the nature of the organic stabilizer system we demonstrate control over the reaction kinetics and hence the shape of the nanostructures. Investigations into the structural evolution of the nanostructures show that they form from multiply twinned face centered cubic (fcc) nanoparticle nuclei. Reaction kinetics then determine the resulting shape where ultrafast growth is shown to lead to the highly branched nanostructures. These results will contribute greatly to the understanding of complex nanoparticle growth from all fcc metals. The nanostructures then show excellent catalytic activity for the hydrogenation of nitrobenzene to aniline.

KEYWORDS: palladium · nanocrystals · nanoparticles · catalysis · X-ray diffraction · electron microscopy

The synthesis of inorganic nanocrystals with controllable morphologies is a key goal in modern materials science and has attracted substantial interest in recent years.[1−4] The shape and size dependent properties of nanoparticles are well established and a fine degree of control over size and morphology can lead to the formation of materials with specific chemical and physical properties. Complex morphologies, in particular, show great promise in many applications as they often exhibit unique electronic, magnetic, photonic, and catalytic properties.[5]

Palladium is well-known for its ability to absorb hydrogen in high concentrations and is a promising material in hydrogen storage and gas sensing applications.[6,7] Nanostructured palladium also shows potential as a surface enhanced Raman spectroscopy (SERS) substrate where the spectral range and intensity enhancement have been shown to be morphology dependent.[8,9]

Palladium is also the most versatile and widely used catalyst in pharmaceutical and fine chemical syntheses.[10] Here, both homogeneous and heterogeneous palladium-based catalysts are required to deliver high selectivities in the desired functional group transformations or couplings. Additionally, palladium serves as an important catalyst for the reduction of harmful exhaust emissions. In this situation, poor accessibility and poisoning of the metal surface can reduce overall efficiency.[11] Therefore, development of high surface area, high performance palladium catalysts is a major concern. To be an economically viable catalyst, the amount of metal consumed in production must be minimized without a reduction in catalytic performance. Highly branched nanostructures are promising candidates as they possess a large surface area available for reaction, while selectively exposing specific (high index) crystal facets.

In the present study we demonstrate the formation of extensively branched palladium nanostructures in a room temperature solution phase synthesis. The synthesis is performed in a pressure reaction vessel (Fischer−Porter bottle) which gives control over atmospheric pressure and composition. This method has previously been shown to be effective for the formation of spherical metal nanoparticles.[12] The use of organic surfactant molecules to control growth is commonly used in nanoparticle synthesis. Here we show that by varying the nature of the organic surfactant system we are able control the growth kinetics and form highly branched nanostructures.

RESULTS

In solution phase nanoparticle synthesis, variation of the organic stabilizer is routinely used to control nanoparticle morphology.[12] Here we demonstrate through two experiments that by changing the sur-

*Address correspondence to Richard.Tilley@vuw.ac.nz.

Received for review September 23, 2009 and accepted December 11, 2009.

Published online December 22, 2009. 10.1021/nn901277k

factant system we can induce structural changes in palladium nanostructures. The first experiment we describe used solely oleylamine as the surfactant. Oleylamine was selected as it has previously been effective for the shape control of platinum nanostructures in the Fischer−Porter bottle.[13,14] The second experiment employed the organic surfactants oleic acid and oleylamine in a 1:1 ratio. The addition of a carboxylic acid functionality has previously been shown to induce shape change in nickel colloids.[15] Both reactions were carried out at room temperature under 3 bar (1 bar = 10^5 Pa) hydrogen for 160 min.

Figure 1a shows a transmission electron microscopy (TEM) image of the reaction product when oleylamine only is used as the surfactant. As can be seen in the image, the nanoparticles consist of nanostructured polyhedra 6 ± 1.5 nm in size. Figure 1b shows a high resolution transmission electron microscopy (HRTEM) image of one of the polyhedra. The particle is characterized as a multiply twinned face centered cubic (fcc) icosahedra viewed along a ⟨112⟩ zone axis.[16,17]

Figure 1c shows a low magnification TEM image of the highly branched palladium nanostructures synthesized in a surfactant system containing a 1:1 ratio of oleic acid and oleylamine. The palladium nanostructures are 85 ± 15 nm in size and each particle displays extensive branching with the branches growing radially away from a central core. The selected area diffraction (SAED) pattern of the nanoparticles observed is shown in the inset and can be readily indexed to the fcc structure of palladium. Figure 1d shows a higher magnification image of a single nanostructure. The particle branches have a broad leaflike structure and exhibit a rounded tip, similar to dendritic growth.[18−20] Flowerlike nanostructures have previously been produced for Pd and Pt; however, these where grown hierarchically from smaller nanoparticle building blocks and hence were covered by low index facets.[21,22]

The above set of experiments illustrates that changing the surfactant system directly affects the nanoparticle shape. The reaction with oleylamine produced polyhedra as shown in Figure 1a,b. Polyhedra are commonly formed for palladium and are widely accepted as a thermodynamically favored morphology.[23,24]

When oleic acid is introduced, in a 1:1 ratio with oleylamine, highly branched nanostructures are formed which possess a high surface area to volume ratio. This presents an interesting result as the formation of these types of highly branched nanostructures terminated by high index facets has not previously been observed for palladium. In solution phase synthesis, palladium nanostructures typically form as thermodynamically favored polyhedra structures or 1-D nanorods.[25−27] The surfaces of these nanostructures are limited to low index facets due to their lower surface−solution interface energy.[28,29]

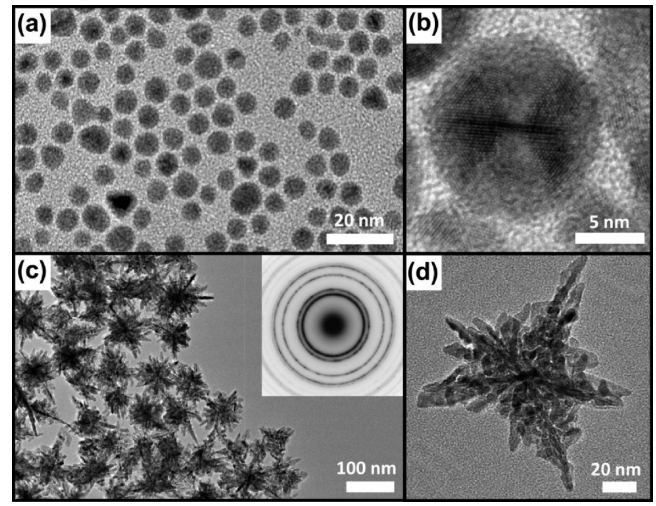

Figure 1. Transmission electron microscopy (TEM) images of palladium nanostructures prepared after 160 min at room temperature: (a) polyhedra nanoparticles formed using purely oleylamine as surfactant, (b) high resolution image of one of the polyhedra nanoparticles characterized as a multiply twinned fcc icosahedra, (c) highly branched nanostructures formed using a 1:1 mixture of oleylamine and oleic acid, and (d) high resolution image of one of the nanostructures.

Thus, by altering the nature of the surfactant system we present a simple solution phase synthesis for the formation of highly branched, high surface area palladium nanostructures.

Time Dependent Reactions. To investigate the mechanism of growth for the highly branched nanostructures intermediates were isolated by varying the reaction time of a 1:1 mixture of oleic acid and oleylamine.

Reaction times were shortened to 20, 30, 80, and 120 min, and images of the individual nanoparticles formed are shown in Figure 2 panels a, b, c, and d, respectively.

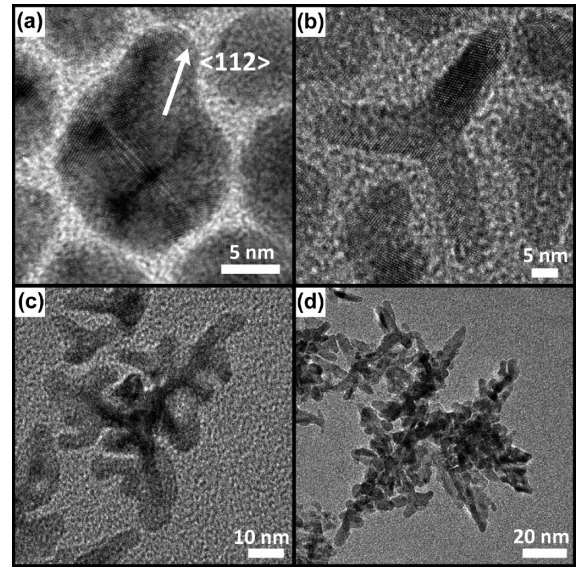

Figure 2. HRTEM images showing the evolution of the highly branched nanostructures: (a) icosahedra with small leg beginning to grow in the [112] direction; (b) tripod-shaped nanoparticle formed after 30 min; (c) intermediate morphology after 80 min; and (d) fully formed nanostructure after 120 min.

A low magnification TEM image of the nanoparticles formed after 20 min is also shown in Supporting Information, Figure S1. The nanoparticles formed after 20 min were predominantly nanoparticles with polyhedra shapes similar to those shown in Figure 1a,b.

Figure 2a (20 min) shows a nanoparticle 14 nm in size. Analysis of the atomic packing indicates this nanoparticle is a multiply twinned fcc icosahedra viewed down a ⟨112⟩ zone axis. This is similar to the nanoparticle seen in Figure 1b except the nanoparticle shown here displays the start of single branched growth in the [112] direction.

Figure 2b (30 min) shows a nanoparticle 45 nm in size which displays a tripod morphology. A tripod morphology forms when arm growth occurs in three symmetry equivalent [112] directions from multiply twinned fcc icosahedra.[30]

The particle in Figure 2c (80 min) is 65 nm in size and retains the tripod backbone with 3-fold symmetry. However, a secondary type of growth has now occurred from the tripod arms. This growth occurs along random crystallographic directions and leads to a broad, leaflike structure.

Figure 2d (120 min) displays a nanoparticle 100 nm in size. The secondary growth has continued at various angles away from the tripod backbone leading to a high surface area branched structure. The final reaction product formed after 160 min was shown in Figure 1d. Extensive branching has occurred along radial directions from the particle core to give a highly branched morphology.

***In-Situ* X-ray Diffraction.** To understand the kinetics of nanoparticle growth for the as synthesized palladium nanostructures, *in situ* synchrotron X-ray diffraction (XRD) experiments were carried out. Since it is difficult to gain information on growth kinetics with post synthetic characterization techniques, *in situ* XRD was needed as a method that can measure structural dynamics in real time. Experiments were performed at the Stanford Synchrotron Radiation Lightsource (SSRL) on beamline 7−2 (see Supporting Information for experimental procedure). These were carried out in a specially made reaction cell shown in Supporting Information, Figure S2.

Figure 3a shows the (111) reflection of palladium tracked over the course of a typical reaction displaying the formation of a crystalline product in a 1:1 reaction with oleic acid and oleylamine. To ensure that the time scale of the reaction better suited synchrotron experiments, the cell temperature was raised to 35 °C; 10 °C above that used to form the nanoparticles used in EM observation. This leads to a slight decrease in reaction times when compared to HRTEM experiments. The full width at half-maximum of the diffraction peak provides a measure of the crystallite size in the nanostructures. This remained relatively constant throughout both experiments, which is consistent with the multiply

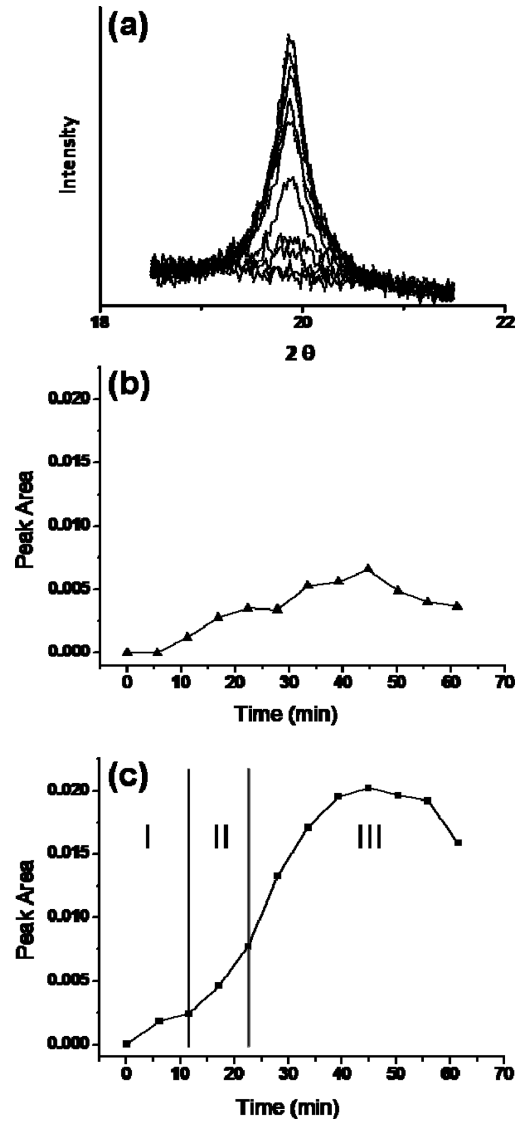

Figure 3. Time resolved synchrotron XRD results tracking the growth of the palladium nanostructures: (a) *in-situ* XRD results showing the evolution of crystalline palladium by tracking the Pd(111) reflection for the 1:1 reaction, (b) peak area *vs* reaction time plot for the 1:0 reaction and (c) for the 1:1 reaction.

twinned nature of the nanostructures. The lattice parameter calculated from the peak positions was independent of reaction time and close to the bulk value indicating little or no lattice strain. However, due to peak broadening and uncertainty in the measurements some undetected strain may be present, particularly at the initial reaction times when the diffraction peak is at its weakest and broadest. The measured diffraction signal is from crystalline nanostructures in solution as there was no deposition of product on the cell window at the completion of the reaction.

To investigate the difference in reaction kinetics between the formation of palladium polyhedra and highly branched nanostructures, experiments in oleylamine and a 1:1 mixture of oleic acid and oleylamine were carried out as shown in Figure 3b,c, respectively. These

both show the continuous growth of the Pd(111) peak area over time.

Figure 3b shows the growth of nanocrystalline palladium to form palladium polyhedra when only oleylamine is used (1:0 reaction). The plot shows a steady, nearly linear increase that reaches a maximum at 45 min. The slope of the growth line is constant which indicates a steady growth rate throughout the experiment. The peak area then decreases as the particles grow too large to remain in suspension and settle out of the beam path.

When a surfactant system containing oleic acid in a 1:1 ratio with oleylamine is employed (1:1 reaction) different growth characteristics emerge (Figure 3c). Here, the growth of the nanostructures progresses in three distinct stages. Stage I shows steady initial growth with a slope similar to the 1:0 case. In Stage II the slope and growth rate increases 2-fold and continues at this rate for 10 min. Stage III shows a further 2-fold increase in growth rate when compared to Stage II. The peak area then begins to decrease as growth ceases and settling occurs.

Growth Mechanism. The above HRTEM and XRD experiments show that the growth and kinetics of formation of highly branched palladium nanostructures are distinctly different to the formation of the palladium polyhedra.

For the 1:0 reaction there is a relatively slow and constant growth rate, as shown in Figure 3b, which results in the polyhedra nanoparticle shapes observed in Figure 1a. This slow, constant growth indicates that for the 1:0 reaction, growth occurs under thermodynamic control to produce thermodynamically favored polyhedra.[31]

In contrast, for the 1:1 reaction (Figure 3c) there are three distinct growth stages leading to the formation of the highly branched nanostructures. Each stage possesses different growth kinetics as described as follows (Stages I−III).

Stage I. The growth rate for Stage I of the 1:1 reaction is relatively slow and comparable to the growth rate of the entire 1:0 reaction. For this stage, HRTEM analysis shows the formation of multiply twinned fcc icosahedral nuclei (Supporting Information, Figure S1). This is the same polyhedra structure formed in the 1:0 reaction (see Figure 1a,b). Therefore, during the slow growth of Stage I of the 1:1 reaction, thermodynamically favored multiply twinned fcc icosahedra nuclei form.

Stage II. During Stage II of the 1:1 reaction there is a 2-fold increase in the growth rate when compared to Stage I. This indicates growth is no longer thermodynamically controlled and kinetically controlled growth conditions are present.[31]

In solution phase synthesis of nanoparticles, kinetically controlled growth conditions can lead to branched growth. This process was observed in Figure 2a with the start of branched growth from a multiply twinned icosahedra nuclei. In our case novel tripod shapes form due to branch growth occurring along three symmetry equivalent [112] directions from the icosahedra nuclei (Figure 2b).[30]

Therefore, as palladium crystallizes in the highly symmetrical fcc crystal structure the formation of a branched shapes requires both a breaking of the crystal symmetry, introduced through defects in the icosahedral nanoparticle nuclei, and growth conditions which are kinetically controlled.

It should be noted that although the nanoparticles in Stage II are now growing under kinetic control, growth is still occurring along selected crystallographic directions.

Stage III. In Stage III there is another 2-fold increase in the growth rate compared to Stage II. This increase follows the formation of the tripod branches and is due to the start of the secondary growth observed in Figure 2c. This secondary growth leads to a "leaflike" structure off the tripod backbone. The growth rate is now four times as fast as in Stage I which indicates this type of secondary growth is fast and kinetically controlled, occurring very far from thermodynamically controlled conditions.

Because of the rapid rate and distinctly kinetic nature of the ultrafast growth, the adatom adsorption rate does not depend on the crystal facet where adsorption occurs. Hence growth occurs along no preferred crystallographic direction.[32] This leads to randomly oriented branch growth occurring in any radial direction away from the particle core to give the highly branched morphology.

In contrast, the extensive branching observed in dendritic nanostructures formed in the solution phase is dependent on crystallographic direction and is typically a result of diffusion limited aggregation or oriented attachment mechanisms.[18−20] The ultrafast kinetic growth described here leads to branching irrespective of the crystal facet. Therefore, this growth provides a route toward the formation of complex nanoparticle shapes from nuclei with any morphology and surface energy.

Following the ultrafast growth (after 45 min, end of stage III) the peak area begins to decline as the nanoparticles settle out of the beam path.

Therefore, from HRTEM and XRD experiments, the formation of the palladium polyhedra nanoparticles is shown to occur through slow, thermodynamically controlled growth. In contrast, formation of the highly branched nanostructures occurs through (i) the formation of multiply twinned *fcc* icosahedra nuclei, (ii) kinetically controlled branch growth to form a tripod backbone, and (iii) ultrafast secondary kinetic growth occurring in any crystallographic direction from the tripod arms.

Effect of Surfactant System on Reaction Kinetics. In the present system, the kinetics of growth, and hence the final particle morphology, are controlled by the surfactant system. The difference in surface stabilization ability of the amine and acid functionalities determines the growth kinetics by controlling the rate of monomer supply to the nanoparticle surface.[33]

When the rate of adatom diffusion across the particle surface to stable positions is faster than the rate of adatom adsorption, growth is thermodynamically controlled and thermodynamically favored morphologies form. Conversely, when adatom adsorption occurs at a faster rate, growth becomes kinetically controlled leading to more complex nanoparticle shapes.[31]

The carboxylic acid functionality of oleic acid possesses a weaker binding strength to palladium compared to the amine functionality of oleylamine.[34,35] Introducing weaker binding oleic acid (1:1 reaction) will reduce the overall degree of surface stabilization of the growing particle by the surfactant system. This allows rapid adatom adsorption and kinetically controlled growth conditions resulting in highly branched structures.

This is in contrast to the 1:0 reaction where oleylamine binds strongly to the surface of the growing particle. Therefore, the icosahedral nuclei experience strong stabilization effects hindering adatom adsorption. Growth conditions are then thermodynamically controlled and thermodynamically favored polyhedral structures are maintained.

An additional experiment was performed to verify the proposed surface capping mechanism. When purely oleic acid is used as surfactant micrometer sized crystallites form; presumably because there is not enough stabilizing ability by oleic acid to restrict growth to the nanoscale for this system (see Supporting Information, Figure S3).

Catalysis. Highly branched nanostructures are ideally suited to catalysis as high surface area and the presence of high index facets lead to increases in catalytic activity. High index facets have a higher density of atomic steps, ledges, kinks, and dangling bonds, all of which often exhibit much higher reaction activities.[36,37]

Here, HRTEM experiments were used to probe the nature of the surface for the highly branched nanostructures. Figure 4a shows an HRTEM image of one of the nanoparticle branches viewed down a ⟨110⟩ direction. A close up of the branch is shown in Figure 4b. Analysis of the atomic packing in Figure 4b confirms the presence of high index facets. The arrows point to atomic vacancies on the branch edge which create a series of alternating (200) and (111) microfacets. These microfacets combine to form the high index (113) facet. This is shown schematically in Figure 4c.

To test the catalytic properties, the palladium nanostructures were supported onto activated carbon and the resulting catalysts (Pd−NS/C) were examined and

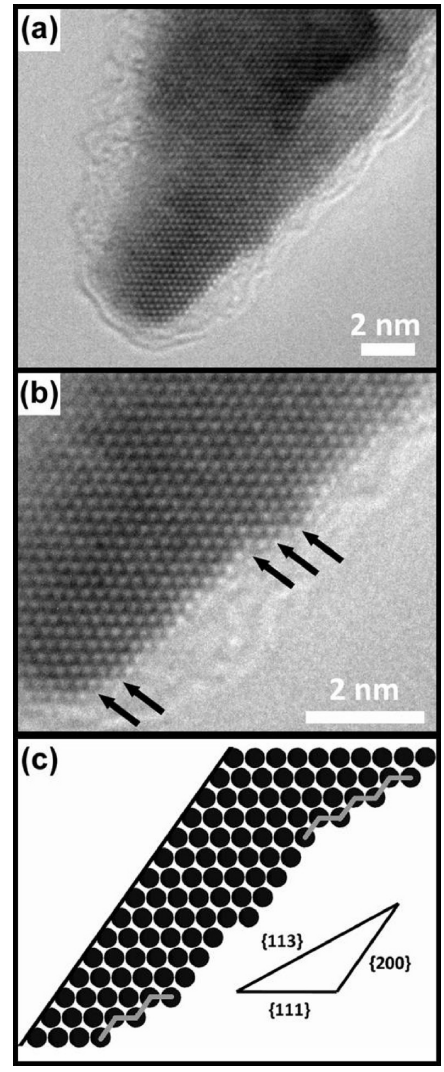

Figure 4. Analysis of the surface of one of the highly branched nanostructures: (a) HRTEM image of one of the particle branches; (b) close-up HRTEM image of the particle branch showing clear atomic packing. The black arrows point to atomic vacancies on the particle surface. (c) Schematic showing how the atomic vacancies lead to high index (113) facets.

compared to commercially available palladium catalysts (Johnson Matthey 1% Pd/C 87 L) for the hydrogenation of nitrobenzene (see Supporting Information for experimental procedure). The catalytic hydrogenation of nitrobenzene to aniline is commonly used as a standard test for the activity of heterogeneous catalyst systems.[38] In addition to this, the reaction has great commercial importance in its own right, in the industrial production of aniline for the polyurethane industry.[39] The carbon-supported palladium was used at a 1:1000 ratio with respect to the substrate, under 2 bar of H_2 at 50 °C in a Buchi pressflow gas-controlled Baskerville autoclave.

The Pd-NS/C material reproducibly showed considerable activity for the hydrogenation of nitrobenzene. After 30 min, there was no further hydrogen uptake, indicating that the reaction had reached completion.

Subsequent analysis by gas chromatography confirmed this, revealing that all of the starting material had been consumed and aniline was the sole product. The formation of intermediate products such as hydroxylamines, oximes, or para-aminophenols was not observed; the presence of which can be observed in less active catalytic systems or those that have been deliberately poisoned.[40]

The commercially available catalyst was also examined under the same reaction conditions. In this case, the reaction was complete within 20 min, again with complete conversion to the desired product. However, with the higher dispersion of this catalyst, this increase in activity is to be expected. What is significant is that the Pd NS/C catalysts display activities nearly the same as that of commercially available analogues, despite the presence of residual oleylamine stabilizing ligands. The novel shapes of the palladium nanostructures offer the possibility of the unique facets to provide alternative selectivities for specific chemoselective reactions. The investigation into such transformations is ongoing.

CONCLUSION

In conclusion, we have synthesized highly branched palladium nanostructures terminated by high index facets in a room temperature solution phase synthesis. By varying the nature of the surfactant system we are able to control the growth kinetics and hence the particle morphology. The highly branched nanostructures grow from multiply twinned fcc icosahedra nuclei *via* a tripod intermediate. A type of secondary ultrafast kinetic growth then occurs from the tripod intermediate along no specific crystallographic direction resulting in highly branched nanostructures.

The palladium nanostructures demonstrate good activity in the hydrogenation of nitrobenzene to aniline where the production of the desired product occurs at a similar rate to commercially available catalysts. The tuning of the morphology of the metal also offers the possibility of varying the selectivity of industrially important organic transformations.

These results and the proposed growth mechanism contribute to the understanding of the formation of highly branched nanostructures from the highly symmetrical fcc crystal structure. The ultrafast kinetic growth observed is not dependent on crystal facet energy and therefore provides a route to complex nanoparticle shapes from any nuclei morphology. The development of a room temperature solution phase synthesis for the formation of highly branched palladium nanoparticles is important for catalytic applications where high surface area and high index facets are known to greatly improve catalytic performance.

EXPERIMENTAL SECTION

Synthesis of Highly Branched Palladium Nanoparticles. In a typical synthesis, 0.1 mmol of palladium precursor (bis(acetonitrile) palladium dichloride, 99%, Aldrich) was added to 1 mL of toluene. To this was added 10 equiv of organic surfactant in total. The palladium precursor was then decomposed under hydrogen in a pressure reaction vessel (Fischer−Porter bottle). Samples were purified by the addition of an equal amount of methanol to flocculate the nanoparticles, use of a centrifuge at 14 000 rpm for collection, and subsequent washing with dichloromethane and toluene. The samples for TEM studies were prepared by resuspending the precipitate in toluene. One drop of toluene suspension was placed on a copper TEM grid and allowed to evaporate in ambient conditions. The TEM images and corresponding diffraction patterns were taken on a JEOL 2010 operated at an acceleration voltage of 200 keV.

Synchrotron X-ray Diffraction (XRD). Experiments were performed at the Stanford Synchrotron Radiation Lightsource (SSRL) on BL7-2 in a specially made reaction cell shown in Supporting Information, Figure S2.[41] The cell was 30 mm high and 20 mm wide and was placed in a ceramic heating block on the beamline. It contained a circular reaction chamber 5 mm in diameter and 1 mm thick which was aligned with the beam. The cell windows were made from X-ray transparent Kapton (polyimide) film. A 50 μL portion of reaction solution was injected into the reaction chamber which was then filled with 3 bar H_2. The experiments were conducted using radiation of $\lambda = 1.0$ Å (12.4 keV). Diffractograms were collected over the Pd(111) peak between 2θ values of 18° and 22°, using step scans of 0.02°/step. Growth of the fcc Pd(111) diffraction peak was observed and monitored every 300 s, for 70 min.

Catalysis. Pd NS/C catalysts were prepared by dissolving Pd NS in toluene, using sonication. The resulting black suspension was stirred at room temperature for 18 h with sufficient activated carbon (1.0 g of activated carbon) to generate a 1% (by weight) Pd NS/C catalyst. After this time, the resulting suspension was filtered, revealing a clear filtrate. The subsequent black solid was thoroughly washed with toluene (100 mL), methanol (100 mL), water (100 mL), and methanol (100 mL) in order to remove any excess ligands present. The solid was then dried in a vacuum oven before use. The Pd NS/C was compared in the hydrogenation of nitrobenzene with 1% Pd/C (Johnson Matthey, 87 L). The test was undertaken using a Baskerville autoclave connected to a Buchi pressflow gas controller. The reaction occurred at 50 °C, under 2 bar of dihydrogen, and stirred at approximately 1000 rpm. In each test, 5 mL of a 0.1 M methanol solution of nitrobenzene (containing 0.1 M of mesitylene) was used with a 1:1000 molar ratio of metal to substrate. Subsequent GC analysis was undertaken using a CPSIL-5 column, with mesitylene as an internal standard.

Acknowledgment. R.D.T. and J.W. gratefully acknowledged financial support from the MacDiarmid Institute and VUW. Portions of this research were carried out at the Stanford Synchrotron Radiation Laboratory, a national user facility operated by Stanford University on behalf of the U.S. Department of Energy, Office of Basic Energy Sciences.

Supporting Information Available: HRTEM image of palladium nanoparticles formed after 20 min; image of Synchrotron reaction cell; and HRTEM image of palladium nanostructures formed using only oleic acid as surfactant. This material is available free of charge *via* the Internet at http://pubs.acs.org.

REFERENCES AND NOTES

1. Murphy, C. J.; San, T. K.; Gole, A. M.; Orendorff, C. J.; Gao, J. X.; Gou, L.; Hunyadi, S. E.; Li, T. Anisotropic Metal Nanoparticles: Synthesis, Assembly, and Optical Applications. *J. Phys. Chem. B* **2005**, *109*, 13857.

2. Jun, Y. W.; Choi, J. S.; Cheon, J. Shape Control of Semiconductor and Metal Oxide Nanocrystals Through Nonhydrolytic Colloidal Routes. *Angew. Chem., Int. Ed.* **2006**, *45*, 3414.
3. Burda, C.; Chen, X. B.; Narayanan, R.; El-Sayed, M. A. Chemistry and Properties of Nanocrystals of Different Shapes. *Chem. Rev.* **2005**, *105*, 1025.
4. Xia, Y.; Xiong, Y. J.; Lim, B.; Skrabalak, S. E. Shape-Controlled Synthesis of Metal Nanocrystals: Simple Chemistry Meets Complex Physics. *Angew. Chem., Int. Ed.* **2009**, *48*, 60.
5. Klabunde, K. J., *Nanoscale Materials in Chemistry*, John Wiley & Sons, 2001.
6. Suleiman, M.; Jisrawi, N. M.; Dankert, O.; Reetz, M. T.; Bahtz, C.; Kirchheim, R.; Pundt, A. Phase Transition and Lattice Expansion During Hydrogen Loading of Nanometer Sized Palladium Clusters. *J. Alloy. Comp.* **2003**, *356*, 644.
7. Pundt, A.; Suleiman, M.; Bahtz, C.; Reetz, M. T.; Kirchheim, R.; Jisrawi, N. M. Hydrogen and Pd-Clusters. *Mater. Sci. Eng., B* **2004**, *108*, 19.
8. Xiong, Y. J.; Wiley, B.; Chen, J. Y.; Li, Z. Y.; Yin, Y. D.; Xia, Y. N. Corrosion-Based Synthesis of Single-Crystal Pd Nanoboxes and Nanocages and Their Surface Plasmon Properties. *Angew. Chem. Int. Ed.* **2005**, *44*, 7913.
9. Younan, X.; McLellan, J. M.; Yujie, X.; Min, H. Surface-Enhanced Raman Scattering of 4-Mercaptopyridine on Thin Films of Nanoscale Pd Cubes, Boxes, and Cages. *Chem. Phys. Lett.* **2006**, *417*, 230.
10. Blaser, H. U.; Indolese, A.; Schnyder, A.; Steiner, H.; Studer, M. Supported Palladium Catalysts for Fine Chemicals Synthesis. *J. Mol. Catal.* **2001**, *173*, 3.
11. Bowker, M. Automotive Catalysis Studied by Surface Science. *Chem. Soc. Rev.* **2008**, *37*, 2204.
12. Ramirez, E.; Jansat, S.; Philippot, K.; Lecante, P.; Gomez, M.; Masdeu-Bulto, A. M.; Chaudret, B. Influence of Organic Ligands on the Stabilization of Palladium Nanoparticles. *J. Organomet. Chem.* **2004**, *689*, 4601.
13. Ren, J. T.; Tilley, R. D. Preparation, Self-Assembly, and Mechanistic Study of Highly Monodispersed Nanocubes. *J. Am. Chem. Soc.* **2007**, *129*, 3287.
14. Ren, J.; Tilley, R. D. Shape-Controlled Growth of Platinum Nanoparticles. *Small* **2007**, *3*, 1508.
15. Bradley, J. S.; Tesche, B.; Busser, W.; Masse, M.; Reetz, R. T. Surface Spectroscopic Study of the Stabilization Mechanism for Shape-Selectively Synthesized Nanostructured Transition Metal Colloids. *J. Am. Chem. Soc.* **2000**, *122*, 4631.
16. Penisson, J. M.; Renou, A. Structure of an Icosahedral Palladium Particle. *Z. Phys. D: At., Mol. Clusters* **1989**, *12*, 113.
17. Penisson, J. M.; Renou, A. Structure of an Icosahedral Palladium Particle. *J. Cryst. Growth* **1990**, *102*, 585.
18. Zhou, P.; Dai, Z. H.; Fang, M.; Huang, X. H.; Bao, J. C.; Gong, J. F. Novel Dendritic Palladium Nanostructure and its Application in Biosensing. *J. Phys. Chem. C* **2007**, *111*, 12609.
19. Wen, X. G.; Xie, Y. T.; Mak, W. C.; Cheung, K. Y.; Li, X. Y.; Renneberg, R.; Yang, S. Dendritic Nanostructures of Silver: Facile Synthesis, Structural Characterizations, and Sensing Applications. *Langmuir* **2006**, *22*, 4836.
20. Xiao, J. P.; Xie, Y.; Tang, R.; Chen, M.; Tian, X. B. Novel Ultrasonically Assisted Templated Synthesis of Palladium and Silver Dendritic Nanostructures. *Adv. Mater.* **2001**, *13*, 1887.
21. Zhang, H. T.; Ding, J.; Chow, G. M. Morphological Control of Synthesis and Anomalous Magnetic Properties of 3-D Branched Pt Nanoparticles. *Langmuir* **2008**, *24*, 375.
22. Yin, Z.; Zheng, H. J.; Ma, D.; Bao, X. H. Porous Palladium Nanoflowers That Have Enhanced Methanol Electro-oxidation Activity. *J. Phys. Chem. C* **2009**, *113*, 1001.
23. Elechiguerra, J. L.; Reyes-Gasga, J.; Yacaman, M. J. The Role of Twinning in Shape Evolution of Anisotropic Noble Metal Nanostructures. *J. Mater. Chem.* **2006**, *16*, 3906.
24. Berhault, G.; Bausach, M.; Bisson, L.; Becerra, L.; Thomazeau, C.; Uzio, D. Seed-Mediated Synthesis of Pd Nanocrystals: Factors Influencing a Kinetic- or Thermodynamic-Controlled Growth Regime. *J. Phys. Chem. C* **2007**, *111*, 5915.
25. Xiong, Y. J.; Cai, H. G.; Yin, Y. D.; Xia, Y. N. Synthesis and Characterization of Fivefold Twinned Nanorods and Right Bipyramids of Palladium. *Chem. Phys. Lett.* **2007**, *440*, 273.
26. Choo, H.; He, B. L.; Liew, K. Y.; Liu, H. F.; Li, J. L. Morphology and Control of Pd Nanoparticles. *J. Mol. Catal.* **2006**, *244*, 217.
27. Xiong, Y. J.; Cai, H. G.; Wiley, B. J.; Wang, J. G.; Kim, M. J.; Xia, Y. N. Synthesis and Mechanistic Study of Palladium Nanobars and Nanorods. *J. Am. Chem. Soc.* **2007**, *129*, 3665.
28. Xiong, Y. J.; Xia, Y. N. Shape-Controlled Synthesis of Metal Nanostructures: The Case of Palladium. *Adv. Mater.* **2007**, *19*, 3385.
29. Tian, N.; Zhou, Z. Y.; Sun, S. G. Platinum Metal Catalysts of High-Index Surfaces: From Single-Crystal Planes to Electrochemically Shape-Controlled Nanoparticles. *J. Phys. Chem. C* **2008**, *112*, 19801.
30. Watt, J. Young, N. Haigh, S. Kirkland, A. Tilley, R. D. Synthesis and Structural Characterization of Branched Palladium Nanostructures. *Adv. Mater.* 2009, in press.
31. Yin, Y.; Alivisatos, A. P. Colloidal Nanocrystal Synthesis and the Organic−Inorganic Interface. *Nature* **2005**, *437*, 664.
32. Lou, X. W.; Yuan, C. L.; Archer, L. A. An Unusual Example of Hyperbranched Metal Nanocrystals and Their Shape Evolution. *Chem. Mater.* **2006**, *18*, 3921.
33. Sau, T. K.; Murphy, C. J. Room Temperature, High-Yield Synthesis of Multiple Shapes of Gold Nanoparticles in Aqueous Solution. *J. Am. Chem. Soc.* **2004**, *126*, 8648.
34. Jun, Y. W.; Lee, J. H.; Choi, J. S.; Cheon, J. Symmetry-Controlled Colloidal Nanocrystals: Nonhydrolytic Chemical Synthesis and Shape Determining Parameters. *J. Phys. Chem. B* **2005**, *109*, 14795.
35. Ahrland, S.; Chatt, J.; Davies, N. R. The Relative Affinities of Ligand Atoms for Acceptor Molecules and Ions. *Quart. Rev.* **1958**, *12*, 265.
36. Ma, Y. Y.; Kuang, Q.; Jiang, Z. Y.; Xie, Z. X.; Huang, R. B.; Zheng, L. S. Synthesis of Trisoctahedral Gold Nanocrystals with Exposed High-Index Facets by a Facile Chemical Method. *Angew. Chem., Int. Ed* **2008**, *47*, 8901.
37. Tian, N.; Zhou, Z. Y.; Sun, S. G.; Ding, Y.; Wang, Z. L. Synthesis of Tetrahexahedral Platinum Nanocrystals with High-Index Facets and High Electro-oxidation Activity. *Science* **2007**, *316*, 732.
38. Gelder, E. A.; Jackson, S. D.; Lok, C. M. A Study of Nitrobenzene Hydrogenation Over Palladium/Carbon Catalysts. *Catal. Lett.* **2002**, *84*, 205.
39. Weissermel, K. Arpe, H. J., *Industrial Organic Chemistry*, 3rd ed.; VCH: Weinheim, Germany, 1997.
40. Gao, J.; Wang, F. D.; Liao, S. J.; Yu, D. R. Selective Hydrogenation of Nitrobenzene to *p*-Aminophenol by the Polymer-Supported Palladium-Based Mono- and Bimetallic Catalyst. *React. Kinet. Catal. Lett.* **1998**, *64*, 351.
41. Cheong, S.; Watt, J.; Ingham, B.; Toney, M. F.; Tilley, R. D. *In Situ* and *ex Situ* Studies of Platinum Nanocrystals: Growth and Evolution in Solution. *J. Am. Chem. Soc.* **2009**, *131*, 14590–14595.